Chapter 4

Electrical Studies in Thin Films of $TiPcCl_2$, $SiPcCl_2$, $SnPcCl_2$ and SnPc

4.1 Introduction

Phthalocyanines (Pcs) are macro cyclic compounds characterized by conjugated bonding, i.e. alternate single and double bonds[1]. π electrons are delocalised and are responsible for conduction in molecules having conjugated bonding. Since the inter-molecular attraction is weak, the conduction band will be narrow and hence the mobility will be small. In general Pcs and metallo-phthalocyanines (MPcs) are classified as p-type semiconductors with low mobility and low carrier concentration[2]. The molecular orbital of different molecules can be treated as isolated and hence the free electrons or carriers of the individual molecules stay in them rather than in between them. However, these electrons can jump or hop from one site to another site due to perturbation caused by the neighbouring molecules.

One of the major considerations for the organic thin films is whether energy band model of conduction is applicable to them or not. This question has been raised originally by Gutmann and Lyons[3] and then by Ahmad and Collins[4]. A common thumb rule in this regard is the use of mobility value of 10^{-4} m^2 V^{-1} s^{-1} above which the band theory is considered applicable and below which hopping type conductivity is

found appropriate. However, Ahmad and Collins [4] have argued that very low mobility values of the order of 10^{-10} m^2 V^{-1} s^{-1} give an electron free path of the orders of magnitude smaller than the intermolecular distance. Various electronic conduction processes are observed in phthalocyanine thin films. At higher temperatures, band conduction is observed and at lower temperatures hopping conduction is observed[5]. The conductivity is controlled by the traps, which are normally associated with crystal imperfections, dislocations, grain boundaries and the surface of the material[6]. Two types of carrier traps are found in phthalocyanines:

(i) traps with discrete energy levels in the forbidden energy gap of the material

(ii) traps with quasi-continuous distribution of energy levels usually having maximum density at the edge of the conduction or valence bands.

The electrical properties of phthalocyanine thin films depend on a number of material parameters including film morphology, which in turn is determined by the parameters, like deposition rate, substrate temperature and post deposition annealing[7,8]. In this work, d.c conductivity measurements are carried out in the planar configuration of $TiPcCl_2$, $SiPcCl_2$, $SnPcCl_2$ and SnPc thin films as a function of film thickness, substrate temperature and post deposition annealing in air and vacuum.

4.2 Theory

The semiconducting properties of crystals are due to thermal excitation, impurities, lattice defects and nonstoichiometry. A pure semiconductor exhibits intrinsic semi conductivity. The electrical properties of crystals are not modified by impurities in the temperature range at which they exhibit intrinsic conductivity. In semiconductors, as the temperature is increased from absolute zero, electrons are thermally excited from the valence band to the conduction band, leaving vacant sites in the valence band called holes. Holes in the valence band and the electrons in the conduction band contribute to the electrical conductivity of semiconductors. The conductivity σ due to the electrons and holes is given by

$$\sigma = (ne\mu_e + pe\mu_h) \qquad 4.2.1$$

where n and μe are the carrier concentration and mobility of electrons, p and μ_h are the corresponding quantities for the holes and e is the electronic charge. The expression for carrier concentration is given by

$$n_i = N_c \exp (E_F - E_C)/k_B T$$

$$p_i = N_V \exp (E_V - E_F)/k_B T \qquad 4.2.2$$

where N_C and N_V are the density of states in the conduction band and valence band, E_C represents the bottom of the conduction band and E_V

the top of the valence band. E_F is the Fermi level, k_B and T are the Boltzmann's constant and absolute temperature respectively.

N_C and N_V are given by

$$N_C = 2(2\pi m_e^* k_B T/h^2)^{3/2}$$

$$N_V = 2(2\pi m_h^* k_B T/h^2)^{3/2} \qquad 4.2.3$$

where m_e^* and m_h^* are the effective masses of the electrons and holes respectively. Employing the fact that $n_i = p_i$, it follows from Eqn. 4.2.2 that

$$E_F = (E_C+E_V)/2 + \tfrac{3}{4}\, k_B T \ln (mh^*/me^*) \qquad 4.2.4$$

Substituting this value of E_F in equation 4.2.2.

$$ni = pi = 2(2\pi k_B T/h^2)^{3/2} (mh^*me^*)^{3/4} \exp\left(\frac{-E_a}{2k_B T}\right)$$

$$= A \exp\left(\frac{-E_a}{2k_B T}\right) \qquad 4.2.5$$

where E_a represents the activation energy and A is a constant.

If we assume that the variation of mobility of the electrons and holes in an electric field with temperature is negligible, then the general relation for the conductivity σ is,

$$\sigma = \sigma_o \exp (-Ea/2k_B T) \qquad 4.2.6$$

where σo is a constant. Such an exponential variation of electrical conductivity is known for semiconductors.

When there is more than one linear region in Ln σ versus 1000/T plot, the charge transport involves various mechanisms. The electrical conductivity in phthalocyanines is due to both hopping of holes and charge transport via extended states. There are localized electronic states (traps) associated with the crystal defects such as chemical impurities, structural disorder and surface states. Multiple donor levels or acceptor levels exist within the forbidden energy gap and deeper levels can be frozen out as the temperature is increased. In such a case the conductivity is given by

$$\sigma = A \exp(-E_1/k_BT) + B \exp(-E_2/k_BT) + C \exp(-E_3/k_BT) + \ldots\ldots \qquad 4.2.7$$

where E_1 is the intrinsic energy gap and E_2, E_3, …….. are the activation energies needed to excite the carriers from the corresponding trap levels to the conduction band and A, B, C are constants. The steady state transport properties of carriers in organic semiconductors are dominated by the presence and energy distribution of carrier trapping sites.

The conductivity σ of a film of resistance *R*, length *l*, breadth *b* and thickness *t* is given by

$$\sigma = l/Rbt \qquad 4.2.8$$

Phthalocyanine thin films have high resistance, where measurements are generally made along the length of the specimen. When the work function of the electrode and the material are the same, the contact is called neutral. In this case there is no accumulation of

charge on the material surface after contact. By applying sufficient voltage to the metal electrode a current will pass through the film. A contact is called ohmic when work function of the material is less than the work function of electrode. In this work, silver coatings are used as ohmic contact electrodes for conductivity measurements. Conduction mechanism in phthalocyanine thin films is rather complex due to the presence of defects, faults, impurities, trapping centers etc.

The d.c conductivity of phthalocyanine thin films do not correspond to a single thermally activated process. According to Davis and Mott[9] conduction in an amorphous material can be adduced to three processes and the total conductivity σ_{total} is the sum of the individual contribution

$$\sigma_{total} = \sigma_{intrinsic} + \sigma_{excitation} + \sigma_{hopping} \qquad 4.2.9$$

Intrinsic excitation corresponds to the process observed in inorganic intrinsic semiconductors. It is based on the assumption of electron and hole production via thermal transition from a valence band to the conduction band, and may also occur in several organic solids. The excitation conductivity is related to the generation of charge carriers due to electrons excited to a localized state. Hopping conduction is related to the generation of additional carriers by the charge carriers hopping between the neighbours in the localized states near the Fermi level region. In all the above processes, it can be seen that a plot of Ln σ against 1000/T will give straight line. However, these three processes dominate at different temperature regions. It is seen

that intrinsic conductivity prevails at high temperature region and hopping process at lower temperature region.

4.3 Experiment

$TiPcCl_2$, $SiPcCl_2$, $SnPcCl_2$ and SnPc in the powder form procured from Sigma-Aldrich Chemical Company Inc., WI, USA are used as the source materials. Thoroughly cleaned micro-glass slides of dimensions 36 mm x 25 mm x 1.2 mm are used as substrates. Substrates are cleaned according to the procedure described in section 2.15. Thin films of $TiPcCl_2$, $SiPcCl_2$, $SnPcCl_2$ and SnPc are deposited onto the glass substrates using a "Hind Hi Vac" vacuum coating unit (Model No. 12 A4) by thermal evaporation technique at a base pressure of 10^{-5} Torr from a molybdenum boat as per the procedure described in section 2.13. The rate of evaporation is adjusted to be 10 - 13 nm per minute. The substrates are kept at a distance of 12 cm from the source.

Thin films are deposited by keeping the substrates at room temperature and also at different higher temperatures using a substrate heater whose temperature is monitored and controlled by an electronic temperature controller attached to a chromel-alumel thermocouple. The thicknesses of the $TiPcCl_2$, $SiPcCl_2$, $SnPcCl_2$ and SnPc thin films are measured using multiple beam interference technique as described in section 2.16. Ohmic contacts are made using evaporated silver electrodes for electrical conductivity measurements.

Thin films deposited at room temperature are subjected to post-deposition annealing at different temperatures in air for one hour in a specially designed furnace provided with a digital temperature controller cum recorder. Samples deposited at room temperature are also annealed in vacuum for one hour in a chamber evacuated to a pressure of 10^{-3} Torr.

A programmable Keithley electrometer (Model No. 617), explained in section 2.19 in the constant current source mode is used for electrical measurements. The samples are mounted on the sample holder of the conductivity cell described in section 2.18. Electrical contacts are made using copper strands of diameter 0.8 mm and are fixed to the film with silver paste. The electrical conductivity of thin films is measured in the temperature range 323 – 538 K by keeping the samples in the film holder of the conductivity cell. The temperature of the sample is measured using a chromel-alumel thermocouple kept in contact with the conducting surface of the sample. In order to avoid any possible contamination, the electrical measurements are done in a subsidiary vacuum of 10^{-3} Torr and in darkness.

4.4 Results and Discussion

4.4.1 Dependence of film thickness

The resistances of $TiPcCl_2$, $SiPcCl_2$, $SnPcCl_2$ and SnPc thin films of different thicknesses deposited at room temperature are measured using the programmable Keithley electrometer within the temperature range 323-538 K. The corresponding electrical conductivity σ is calculated knowing the length, breadth and thickness of the film. The activation energies are estimated from the slopes of the plot of Ln σ versus 1000/T. The calculated error in the determination of activation energy is $\pm$ 0.01eV.

Figure 4.4.1.1 shows dependence of Ln σ on temperature of as-deposited $TiPcCl_2$ films of different thicknesses. As seen from the figure, there are two linear parts with different slopes. The change in the slope corresponds to change in activation energy, which implies that different conduction mechanism are involved in electrical conductivity[10,11]. The activation energies E_1 and E_2 for the thicknesses 300 nm, 450 nm and 700 nm are estimated and collected in Table 4.4.1.1. The activation energies E_1 and E_2 of $TiPcCl_2$ thin films decreases with an increase in the film thickness. As the film thickness increases polycrystalline deposits tend to be more and more orderly which causes the reduction in the activation energy.

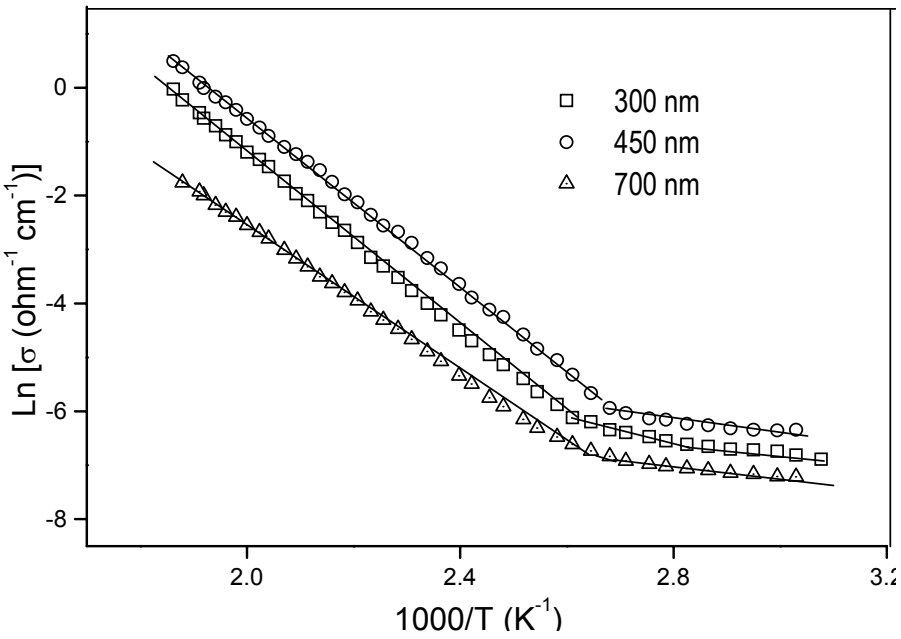

Figure 4.4.1.1 Ln σ versus 1000/T for $TiPcCl_2$ thin films for different thicknesses.

Table 4.4.1.1 Variation of activation energy for $TiPcCl_2$ thin films for different thicknesses.

Thickness (nm)	Activation energy (eV)	
	E_1	E_2
300	0.71	0.08
450	0.66	0.06
700	0.60	0.05

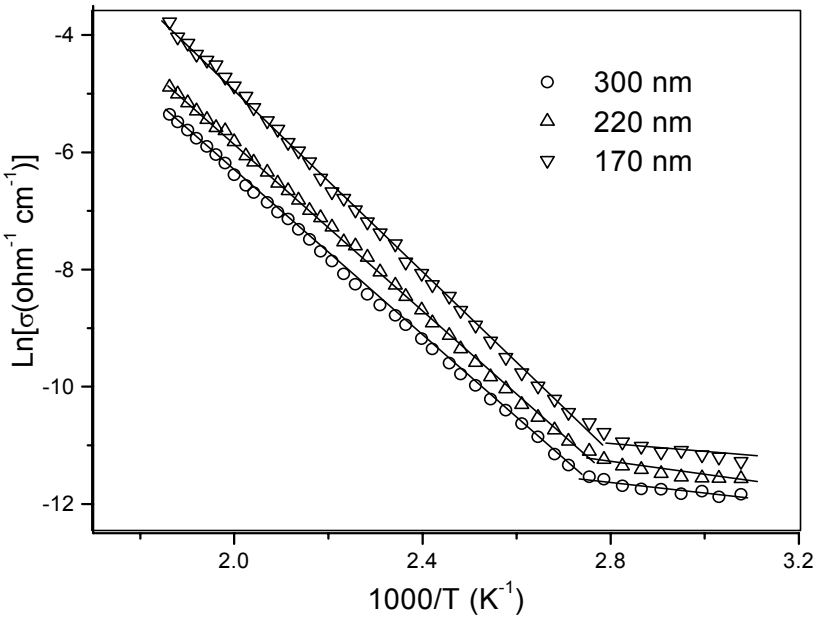

Figure 4.4.1.2 Ln σ versus 1000/T for $SiPcCl_2$ thin films for different thicknesses

Table 4.4.1.2 Variation of activation energy for $SiPcCl_2$ thin films for different thicknesses

Thickness (nm)	Activation energy (eV)	
	E_1	E_2
170	0.67	0.09
220	0.62	0.07
300	0.60	0.05

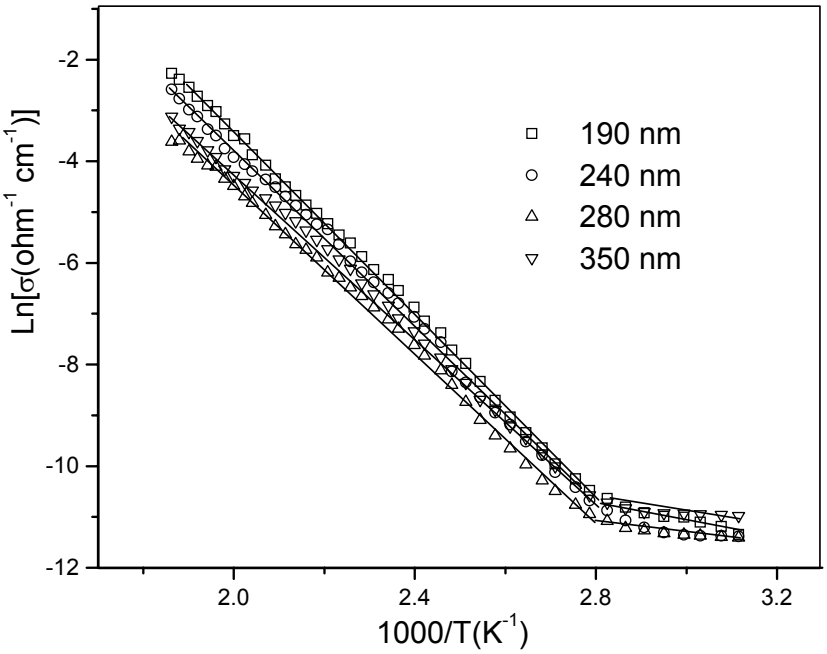

Figure 4.4.1.3 Ln σ versus 1000/T for $SnPcCl_2$ thin films for different thicknesses.

Table 4.4.1.3 Variation of activation energy for $SnPcCl_2$ thin films for different thicknesses.

Thickness (nm)	Activation energy (eV)	
	E_1	E_2
190	0.80	0.15
240	0.76	0.10
280	0.75	0.07
350	0.70	0.06

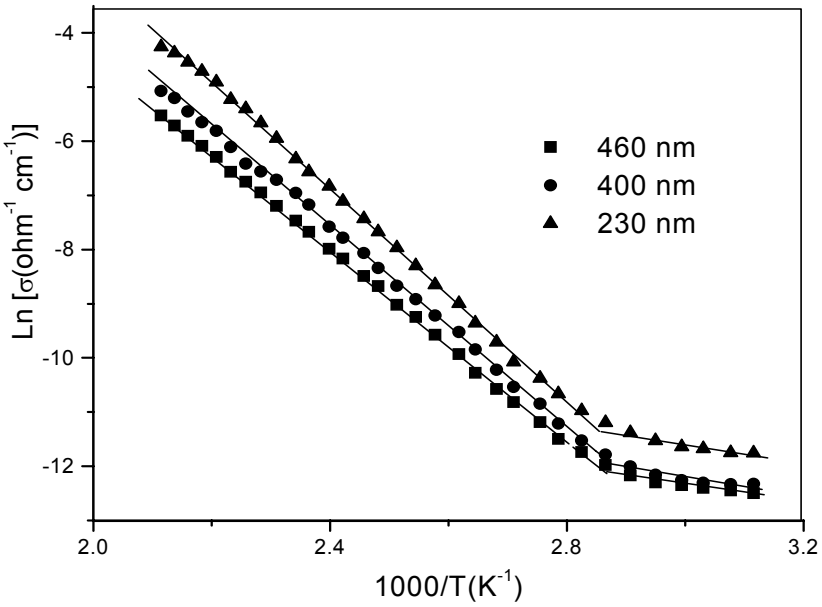

Figure 4.4.1.4 Ln σ versus 1000/T for SnPc thin films for different thicknesses.

Table 4.4.1.4 Variation of activation energy for SnPc thin films for different thicknesses.

Thickness (nm)	Activation energy (eV)	
	E_1	E_2
230	0.85	0.15
400	0.80	0.09
460	0.78	0.08

Figures 4.4.1.2, 4.4.1.3 and 4.4.1.4 show the plot Ln σ versus 1000/T for $SiPcCl_2$, $SnPcCl_2$ and SnPc thin films respectively for different

thicknesses. All the graphs consist of two linear regions, giving two different activation energies. From the slopes of linear regions, the activation energies are estimated for $SiPcCl_2$, $SnPcCl_2$ and SnPc thin films and are collected in Tables 4.4.1.2, 4.4.1.3 and 4.4.1.4 respectively. As shown by the tables, the activation energies E_1 and E_2 of the materials decrease with the increase of thickness. This type of behaviour was reported for H_2Pc and CoPc[12,13]. The activation energy due to thermal excitation is inversely proportional to average linear dimension of the crystallites. As the thickness of the film increases, crystallite size of the film increases which causes the reduction in the intrinsic activation energy[14]. Thicker films often develop surface asperities and defects, which produces decrease in extrinsic activation energy. The central metal ion in MPcs strongly influences the activation energy as well as the mobility in phthalocyanines. Conduction can be described by band theory at higher temperature, whereas it is more appropriate to use hopping mechanism at lower temperature [15].

4.4.2 Dependence of air annealing

For the study of effect of air annealing on the activation energy and conduction mechanism, $TiPcCl_2$, $SiPcCl_2$, $SnPcCl_2$ and SnPc thin films are annealed in air for one hour at 373 K, 423 K, 473 K and 523 K. The resistances of the films are measured at various temperatures using Keithley programmable electrometer in the temperature range 323 K - 538 K. Electrical conductivity is calculated using the equation 4.2.8.

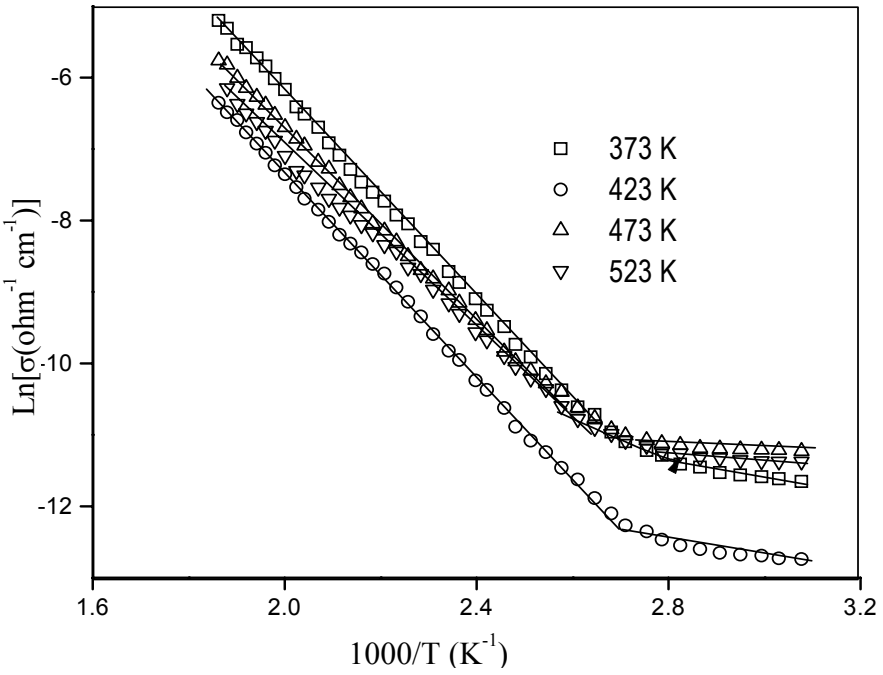

Figure 4.4.2.1 Plot of Ln σ versus 1000/T for $TiPcCl_2$ thin films annealed in air at different temperatures

Table 4.4.2.1. Variation of activation energy for $TiPcCl_2$ thin films annealed in air at different temperatures

Annealing Temperature (K)	Activation energy (eV)	
	E_1	E_2
373	0.62	0.09
423	0.61	0.06
473	0.57	0.03
523	0.52	0.02

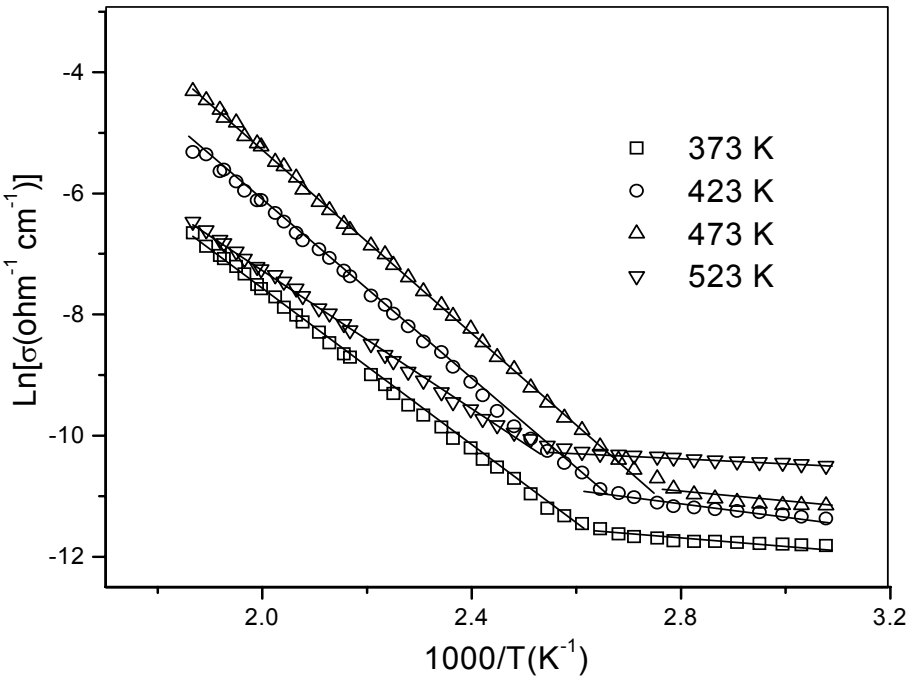

Figure 4.4.2.2 Plot of Ln σ versus 1000/T for $SiPcCl_2$ thin films annealed in air at different temperatures.

Table 4.4.2.2. Variation of activation energy for $SiPcCl_2$ thin films annealed in air at different temperatures.

Annealing Temperature(K)	Activation energy (eV)	
	E_1	E_2
373	0.57	0.04
423	0.64	0.08
473	0.66	0.10
523	0.52	0.04

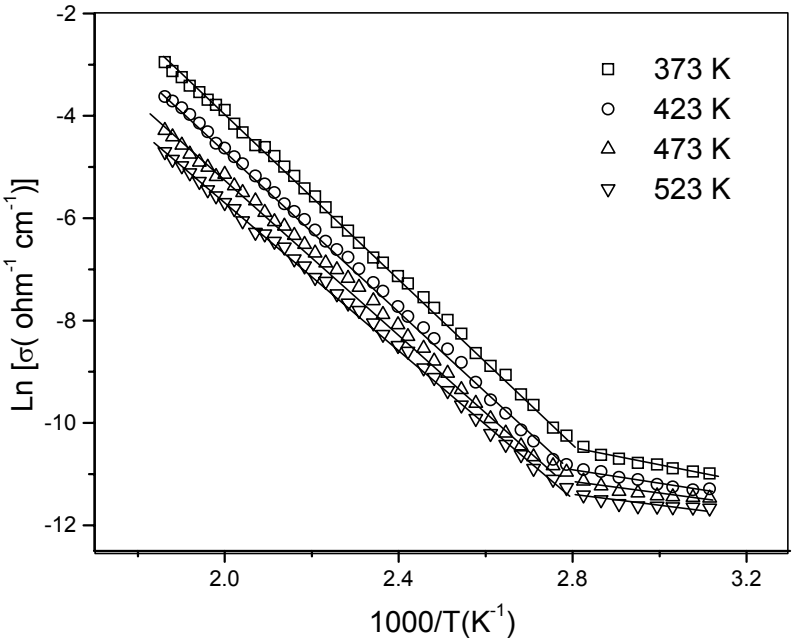

Figure 4.4.2.3 Plot of Ln σ versus 1000/T for $SnPcCl_2$ thin films annealed in air at different temperatures.

Table 4.4.2.3. Variation of activation energy for $SnPcCl_2$ thin films annealed in air at different temperatures.

Annealing Temperature(K)	Activation energy (eV)	
	E_1	E_2
373	0.69	0.15
423	0.68	0.13
473	0.65	0.09
523	0.62	0.08

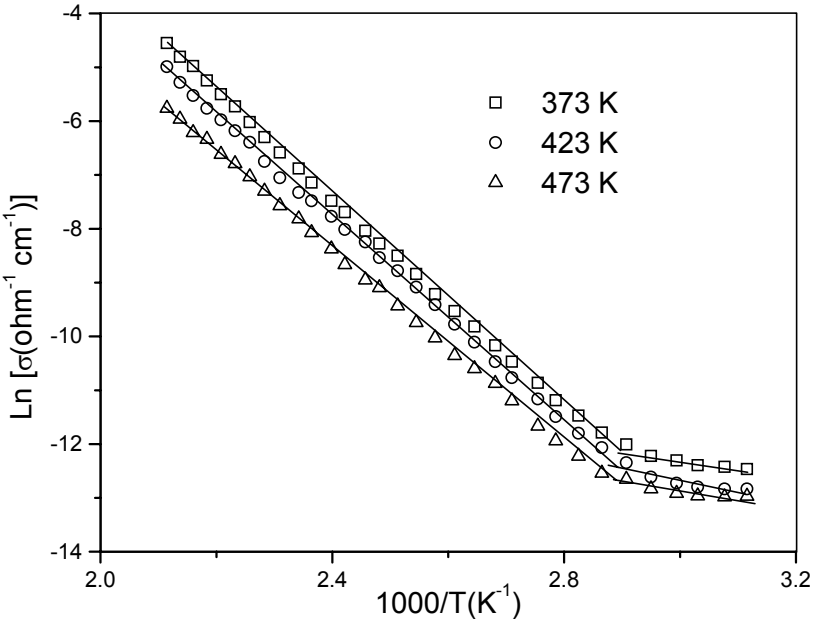

Figure 4.4.2.4 Plot of Ln σ versus 1000/T for SnPc thin films annealed in air at different temperatures.

Table 4.4.2.4. Variation of activation energy for SnPc thin films annealed in air at different temperatures.

Annealing Temperature(K)	Activation energy (eV)	
	E_1	E_2
373	0.84	0.13
423	0.81	0.11
473	0.79	0.07

Figure 4.4.2.1 gives the Ln σ versus 1000/T plots for $TiPcCl_2$ thin films of thickness 500 nm annealed in air at different temperatures. The graph shows two linear regions for each sample. The corresponding activation energies are calculated and given in Table 4.4.2.1. It is observed that activation energy E_1 corresponding to the higher temperature region decreases with an increase in annealing temperature. Since oxygen is known to act as an acceptor center for most of the phthalocyanines[16,17], the variation is explained in terms of oxygen absorption resulting in higher carrier concentration. Therefore electrical conductivity increases and the activation energy decreases[18]. It is seen that intrinsic activation energy E_1 decreases from 0.61eV to 0.52eV as the annealing temperature increases from 373 K to 523 K. The variation in extrinsic activation energy due to annealing can be attributed to the distribution of trapping sites[19]. Similar variation is reported for CuPc thin films[20]. Figure 4.4.2.2 shows the plot of Ln σ versus 1000/T for the $SiPcCl_2$ thin films of thickness 300 nm annealed in air for one hour at 373K, 423 K, 473 K and 523 K. The thermal activation energies corresponding to the two linear regions are estimated and collected in Table 4.4.2.2. It is seen that the intrinsic activation energy E_1 increases with annealing temperature up to 473 K and then it decreases. The increase in E_1 can be attributed to better film ordering due to air annealing. A similar variation in activation energy has been reported in the case of MgPc, NiPc and InPcCl thin films [21-23]. The decrease in E_1 at 523 K indicates that the material itself is unstable at that temperature. Figures

4.4.2.3 and 4.4.2.4 show respectively, the plot of Ln σ versus 1000/T for $SnPcCl_2$ and SnPc thin films annealed in air. The activation energies corresponding to the two linear regions are estimated and are collected in Tables 4.4.2.3 and 4.4.2.4 for $SnPcCl_2$ and SnPc respectively. For these thin films also, the activation energy decrease with the increase of annealing temperature. Because of oxygen absorption, electrical conductivity increases and hence the activation energy decreases.

4.4.3 Dependence of vacuum annealing

To study the effect of vacuum annealing on the activation energy and conduction mechanism, $TiPcCl_2$, $SiPcCl_2$, $SnPcCl_2$ and SnPc thin films are annealed in vacuum of 10^{-3} Torr for one hour at different temperatures. The resistances of the films are measured at various temperatures using Keithley programmable electrometer in the temperature range 323 K to 538 K. Electrical conductivities are calculated using the equation 4.2.8.

Figure 4.4.3.1 shows the plot of Ln σ versus 1000/T for $TiPcCl_2$ thin films of thickness 250 nm annealed in vacuum at 373 K, 423 K, 473 K and 523 K. All the graphs exhibit two linear regions, implying that two different mechanisms are playing an important role in the electrical conductivity. The estimated values of thermal activation energies are given in Table 4.4.3.1. The intrinsic activation energy increases from 0.83 eV to 0.95 eV for an increase of annealing temperature from 373 K to 523 K.

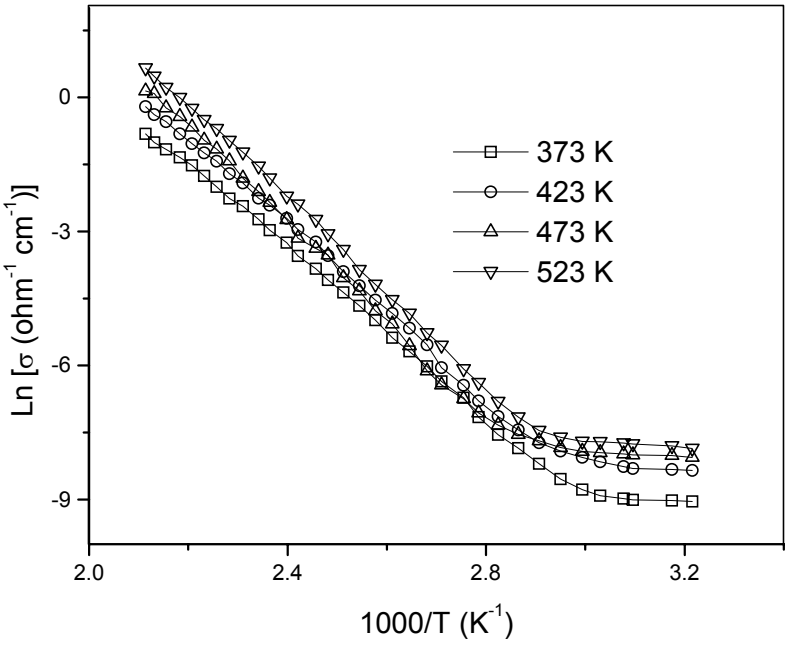

Figure 4.4.3.1 Plot of Ln σ versus 1000/T for $TiPcCl_2$ thin films of thickness 250nm annealed in vacuum at different temperatures.

Table 4.4.3.1. Variation of activation energy for $TiPcCl_2$ thin films of thickness 250nm annealed in vacuum at different temperatures.

Annealing Temperature(K)	Activation energy (eV)	
	E_1	E_2
373	0.83	0.05
423	0.86	0.08
473	0.92	0.08
523	0.95	0.10

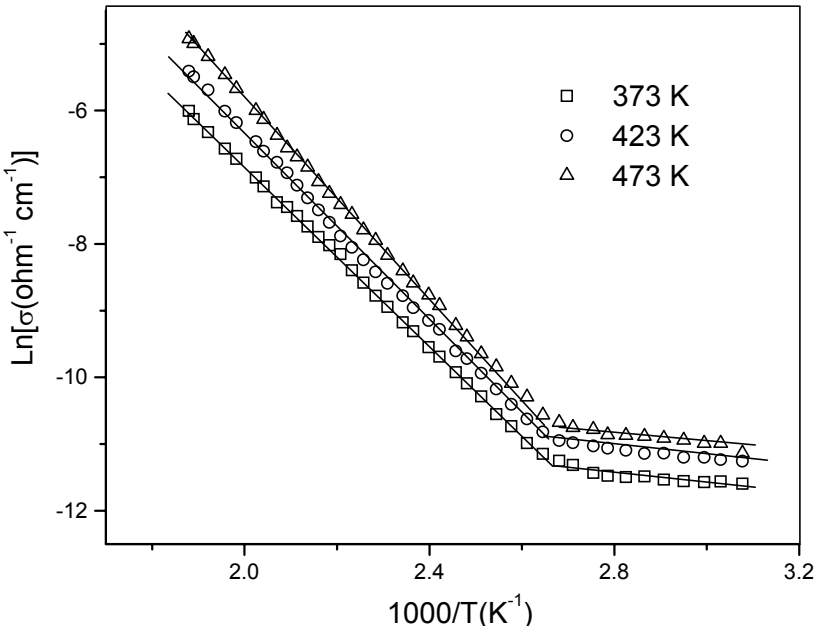

Figure 4.4.3.2 Plot of Ln σ versus 1000/T for $SiPcCl_2$ thin films of thickness 400nm annealed in vacuum at different temperatures.

Table 4.4.3.2. Variation of activation energy for $SiPcCl_2$ thin films of thickness 400nm annealed in vacuum at different temperatures.

Annealing Temperature (K)	Activation energy (eV)	
	E_1	E_2
373	0.58	0.05
423	0.61	0.06
473	0.64	0.08

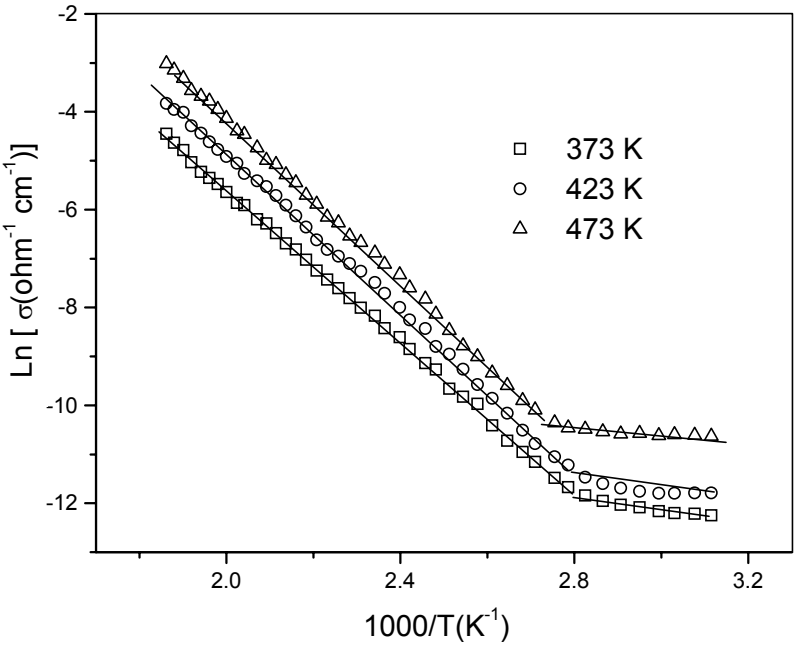

Figure 4.4.3.3 Plot of Ln σ versus 1000/T for $SnPcCl_2$ thin films of thickness 365nm annealed in vacuum at different temperatures.

Table 4.4.3.3. Variation of activation energy for $SnPcCl_2$ thin films of thickness 365nm annealed in vacuum at different temperatures.

Annealing Temperature(K)	Activation energy (eV)	
	E_1	E_2
373	0.68	0.09
423	0.70	0.10
473	0.72	0.08

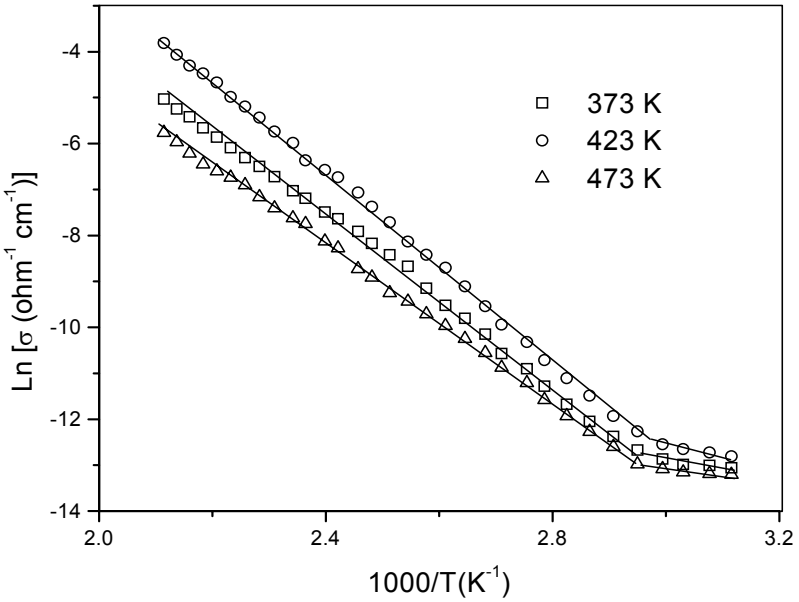

Figure 4.4.3.4 Plot of Ln σ versus 1000/T for SnPc thin films of thickness 400nm annealed in vacuum at different temperatures.

Table 4.4.3.4. Variation of activation energy for SnPc thin films of thickness 400nm annealed in vacuum at different temperatures.

Annealing Temperature(K)	Activation energy (eV)	
	E_1	E_2
373	0.86	0.16
423	0.95	0.18
473	0.77	0.10

The desorption of oxygen which is considered to be a major source of intrinsic conductivity, causes an increase in resistance of the material. Thus the electrical conductivity decreases and hence the activation energy increases[24].

Figures 4.4.3.2 and 4.4.3.3 show the plot of Ln σ versus 1000/T for $SiPcCl_2$ and $SnPcCl_2$ thin films annealed at 373 K, 423 K and 473 K respectively. All the plots exhibit two linear regions giving two activation energies. The estimated values of activation energies for $SiPcCl_2$ thin films of thickness 400 nm and $SnPcCl_2$ thin films of thickness 365 nm are collected in Tables 4.4.3.3 and 4.4.3.4 respectively. These films also show an increase of activation energies with annealing temperatures. A similar behaviour was reported for InPcCl by Samuel *et.al*[23]. For $SnPcCl_2$ thin films annealed at 473 K, there is an increase in extrinsic conductivity due to the appearance of crystal defects as suggested by Amar *et.al*[25]. Trap levels can alter significantly the charge transport in organic semiconductors [26]. Figure 4.4.3.4 shows the plots of Ln σ versus 1000/T for SnPc thin films of thickness 400 nm vacuum annealed at 373 K, 423 K and 473 K. As-deposited samples may contain different levels of defects such as vacancies, grain boundaries and dislocations which can be partially annealed by heat treatment resulting in the decrease in the density of defects and local structural rearrangements, leading to improved crystallinity[27]. Decrease in

activation energy observed for SnPc thin film annealed at 473 K, shows the initialization of starting of phase transition of the material.

4.4.4 Dependence of substrate temperature

The substrate temperature during deposition is perhaps the most critical parameter determining the structure and properties of thin solid films produced by the techniques of vacuum evaporation[28]. To study the variation in activation energy with substrate temperature, Arrhenius plots of Ln σ versus 1000/T are used for films deposited at different substrate temperatures. Thin films of $TiPcCl_2$, $SiPcCl_2$, $SnPcCl_2$ and SnPc are deposited onto purely cleaned glass substrates maintained at temperatures 373 K, 423 K and 473 K. The resistances of the films are measured at various temperatures using Keithley programmable electrometer in the temperature range 323 K to 538 K. The measurements are done in a vacuum of 10^{-3} Torr. Electrical conductivities are calculated using the equation 4.2.8.

Figure 4.4.4.1 shows the plot of Ln σ versus 1000/T for $TiPcCl_2$ thin films of thickness 550 nm deposited at substrate temperatures 305 K, 373 K, 423 K and 473 K. The graph shows two linear regions, indicating a change in conduction mechanism. The activation energy corresponding to these are estimated and collected in Table 4.4.4.1. The intrinsic activation energy decreases with increase of substrate temperature. A sharp decrease is observed for an increase of substrate temperature from 423 K to 473 K. The decrease in activation energy with an increase of substrate temperature may be attributed to an increase in the size of the critical nucleus [29].

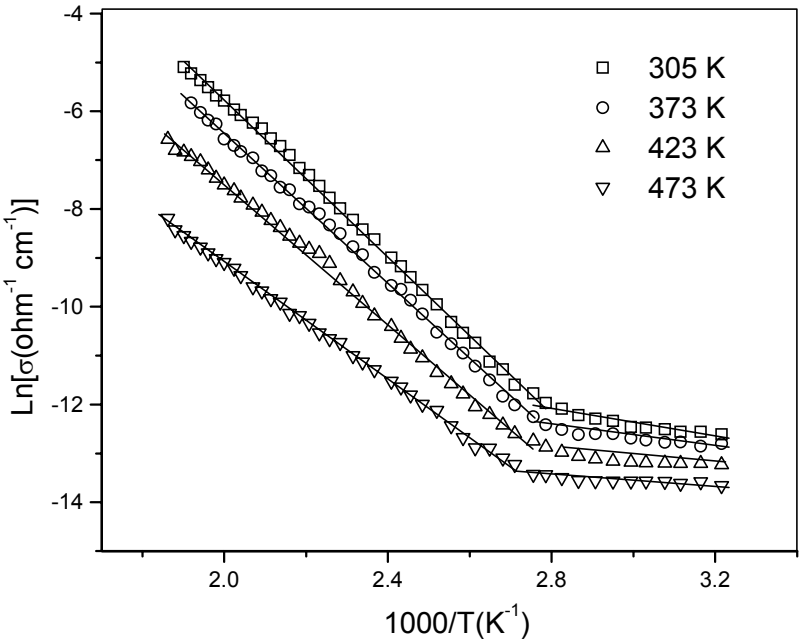

Figure 4.4.4.1 Plot of Ln σ versus 1000/T for $TiPcCl_2$ thin films of thickness 550nm deposited at different substrate temperatures.

Table 4.4.4.1. Variation of activation energy for $TiPcCl_2$ thin films of thickness 550nm deposited at different substrate temperatures.

Substrate Temperature(K)	Activation energy (eV)	
	E_1	E_2
305	0.69	0.09
373	0.66	0.07
423	0.62	0.06
473	0.50	0.03

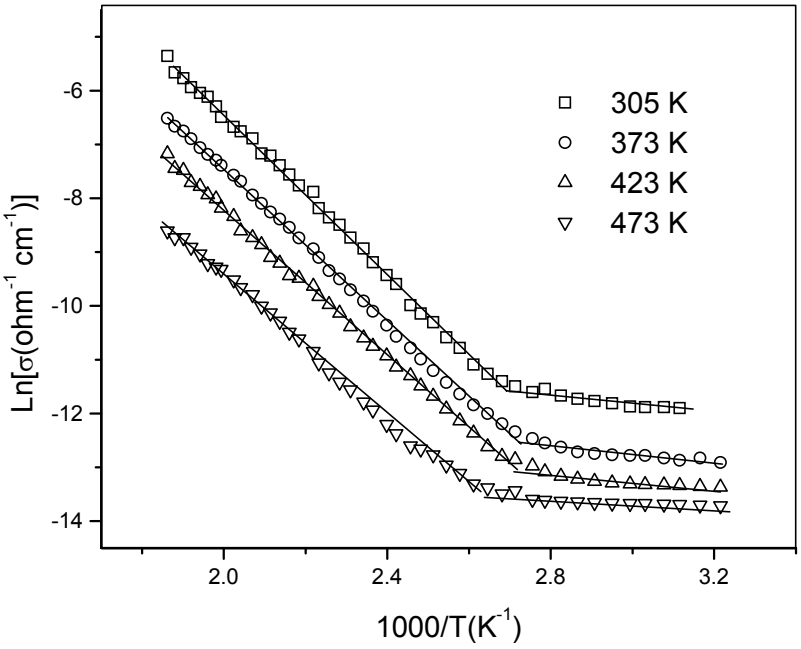

Figure 4.4.4.2 Plot of Ln σ versus 1000/T for $SiPcCl_2$ thin films of thickness 180nm deposited at different substrate temperatures.

Table 4.4.4.2. Variation of activation energy for $SiPcCl_2$ thin films of thickness 180nm deposited at different substrate temperatures.

Substrate Temperature(K)	Activation energy (eV)	
	E_1	E_2
305	0.65	0.08
373	0.63	0.05
423	0.59	0.04
473	0.56	0.02

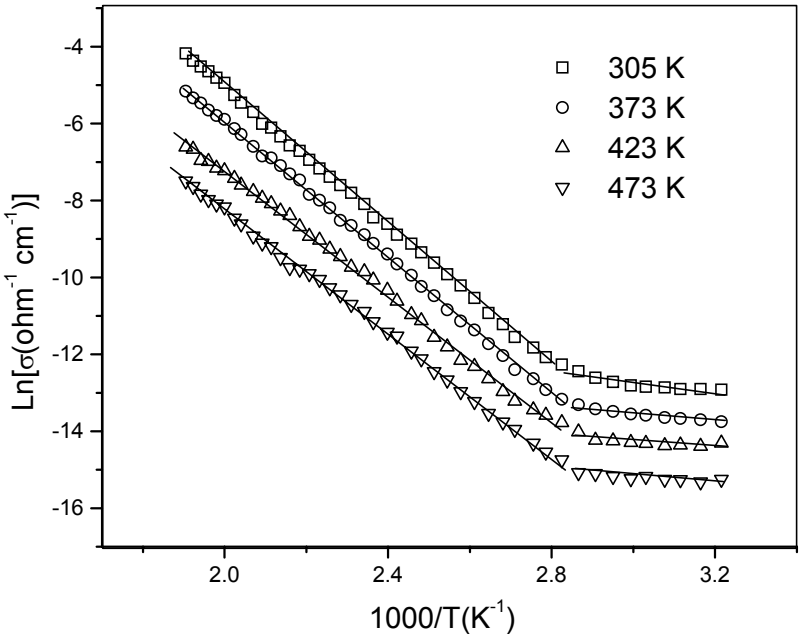

Figure 4.4.4.3 Plot of Ln σ versus 1000/T for $SnPcCl_2$ thin films of thickness 270nm deposited at different substrate temperatures.

Table 4.4.4.3. Variation of activation energy for $SnPcCl_2$ thin films of thickness 270nm deposited at different substrate temperatures.

Substrate Temperature(K)	Activation energy (eV)	
	E_1	E_2
305	0.77	0.11
373	0.76	0.09
423	0.71	0.06
473	0.69	0.05

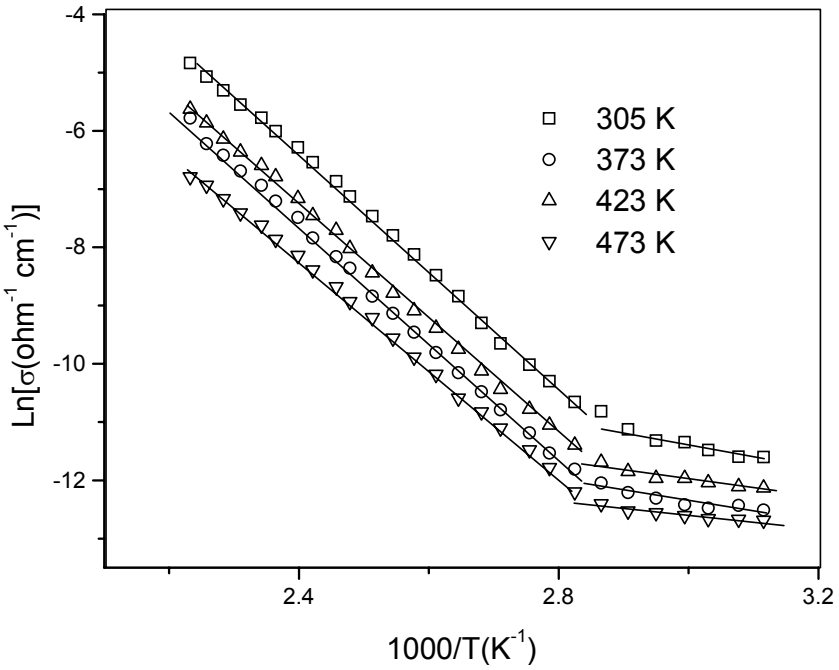

Figure 4.4.4.4 Plot of Ln σ versus 1000/T for SnPc thin films of thickness 250nm deposited at different substrate temperatures.

Table 4.4.4.4. Variation of activation energy for SnPc thin films of thickness 250nm deposited at different substrate temperatures.

Substrate Temperature (K)	Activation energy (eV)	
	E_1	E_2
305	0.87	0.17
373	0.88	0.14
423	0.85	0.11
473	0.80	0.09

Figures 4.4.4.2 and 4.4.4.3 show the Arrhenius plots (Ln σ versus 1000/T) for $SiPcCl_2$ thin film of thickness 180 nm and $SnPcCl_2$ thin films of thickness 270 nm deposited at different substrate temperatures. All the plots show two linear regions, giving two activation energies and are collected in Tables 4.4.4.2 and 4.4.4.3. In both cases, the activation energies decrease with increase of substrate temperatures. This may also be attributed to an increase in the size of the critical nucleus during the film deposition at higher substrate temperature. The Arrhenius plots for SnPc thin films of thickness 250 nm deposited at substrate temperatures 305 K, 373 K, 423 K and 473 K are given in figure 4.4.4.4. The activation energy corresponding to the two linear parts are estimated from the graph and are given in Table 4.4.4.4. There is not much variation in activation energy for SnPc thin films for an increase of substrate temperature from 305 K to 423 K, indicating that there is no notable increase in size of the critical nucleus in this range. But further increase shows a sharp decrease in activation energy.

4.5 Conclusion

Thin films of $TiPcCl_2$, $SiPcCl_2$, $SnPcCl_2$ and SnPc are prepared by thermal evaporation technique and their electrical conductivity studies are made. The dependence of activation energy on film thickness, post deposition annealing in air and vacuum and on substrate temperature are studied. The Arrhenius plots, Ln σ versus 1000/T for $TiPcCl_2$, $SiPcCl_2$, $SnPcCl_2$ and SnPc thin films show more than one linear parts, which

confirms the existence of trap levels. The change in the slope and hence in the activation energy is interpreted as a change from extrinsic to intrinsic conduction. The thermal activation energy E_1 in the higher temperature region is associated with intrinsic conductivity and E_2 in the lower temperature region is associated with impurity conduction. In MPcs, the intrinsic conductivity is due to the partial charge transfer from phthalocyanine ring to the central metal ion. The central metal ion greatly influences the conductivity of MPcs.

In the case of $TiPcCl_2$, $SiPcCl_2$, $SnPcCl_2$ and SnPc thin films, it is observed that increase of film thickness produces a decrease in activation energy. Increase of film thickness may increase the size of micro crystallites and hence a decrease in intrinsic activation energy.

$TiPcCl_2$, $SnPcCl_2$ and SnPc films annealed in air show a decrease of activation energy with an increase of annealing temperature. But for $SiPcCl_2$ thin films, the activation energy increases with increase of annealing temperature up to 473K and the film show instability above 473K. Absorption of oxygen which is acting as acceptor centers for most of the Pcs produce an increase in conductivity and hence a decrease in intrinsic activation energy due to air annealing. But for $SiPcCl_2$ thin films, an increase of activation energy due to better film ordering is obtained due to annealing. For $TiPcCl_2$, $SiPcCl_2$, $SnPcCl_2$ and SnPc thin films, annealing in vacuum produces desorption of oxygen from it. These in turn decrease the conductivity and hence increase in activation

energy. For SnPc, decrease in activation energy observed for annealing at 473 K, shows the initialization of starting of phase transition of the material. Trap levels alter significantly the electrical conduction in $TiPcCl_2$, $SiPcCl_2$, $SnPcCl_2$ and SnPc thin films.

For $TiPcCl_2$, $SiPcCl_2$, $SnPcCl_2$ and SnPc, an increase of substrate temperature results in decrease in activation energy. The studies on the XRD of the samples also support this. $TiPcCl_2$ films show remarkable decrease in intrinsic activation energy in the substrate temperature range 423 K to 473 K. $TiPcCl_2$ thin films are unique in the sense that they are more thermally stable compared to $SiPcCl_2$, $SnPcCl_2$ and SnPc thin films.

References

1. Hans Meier, Organic Semiconductors: Dark and Photoconductivity of Organic Solids, Verlag Chemie, Weinheim, (1974).

2. R. D. Gould, *Co-ord. Chem. Rev.*, **156**(1996) 237.

3. F. Gutman and L. E. Lyons, Organic Semiconductors, Wiley, New York, (1967).

4. A. Ahmad and R. A. Collins, *Thin Solid Films,* **217**(1992) 75.

5. S. I. Shihub and R. D. Gould, *Thin Solid Films,* **254**(1995)187.

6. F. Gutman and L. E. Lyons, Organic Semiconductors A, Krieger, Malabar, (1981).

7. R. A. Collins and A. Belgachi, *Mater. Lett.*, **9**(1989)349.

8. R. A. Collins, K. R. Strickland, M. J. Jeffery, K. Davison and T. A. Jones, *Mater. Lett.,***10**(1990)170.

9. A. Goswami. Thin film fundamentals, New Age international publications, p.500.

10. J. Simon, J. J. Andre, Molecular Semiconductors, Springer, New York, (1985).

11. G. H. Heilmeier and S. E. Harrison, *Phys. Rev.*, **132**(1963)2010.

12. M. M. El-Nahass, A. M. Farid, A. A. Attia and H. A. M. Ali, *Egpt. J. Solids*, **28**(2005) 217.

13. S. Ambily and C. S. Menon, *Thin Solid Films*, **347**(1999)284.

14. A. K. Hassan, R. D. Gould and A. K. Ray, *Phys. Stat. Sol(a),* **158**(1996)K23.

15. M. E. Azim-Araghi, D. Campbell, A. Krier and R. A. Collins, *Semicond. Sci.Technol.*, **11**(1996)39.

16. J. D. Wright, *Prog.Surf.Sci.*, **31**(1989)1.

17. A. M. Saleh, A. K. Hassan and R. D. Gould, J. *Phys. Chem. Sol.*, **64** (2003) 1279.

18. A. K. Hassan and R. D. Gould, J. *Phys.: Condens. matter,* **1**(1989) 6679.

19. A. Sussman, *J.Appl.Phys.*, **38**(1976)2748.

20. S. Ambily and C. S. Menon, *Thin Solid Films*, **347**(1999)284.

21. K. P. Krishnakumar and C. S. Menon, *Ind. J. Pure & Appl. Phys.*, **36**(1998)342.

22. K. N. N. Unni and C. S. Menon, *Mater. Lett.*, **45**(2000)326.

23. Mammen Samuel, C.S.Menon and N.V.Unnikrishnan, *Mater. Sci.* Poland, **23**(2005)707.

24. A. K. Hassan and R. D. Gould, *Int.J. Electron.*, **69**(1990)11.

25. N. Amar, R. D.Gould and A. M. Saleh, *Vacuum.*, **50**(1998)53.

26. N. Karl, Defect control in semiconductors, Elsevier, North Holland, Amsterdam, (1990).

27. A. S. Md. S. Rahman, M. H. Islam and C. A. Horath, *Int.J.Electron.*, **62**(1987)167.

28. P. S. Vincett, W. A. Barlow and G. G. Roberts, J.*Appl.Phys.*, **48**(1977)3800.

29. Milton Ohring, The Material Science of Thin Films, Academic Press, New York (1992).